Electronic and geometrical structure of rutile surfaces

P. Reinhardt and B. A. Heβ
Institut für Physikalische und Theoretische Chemie der Universität Bonn, Wegelerstraße 12, D-53115 Bonn, Germany
(Received 9 May 1994)

The periodic Hartree-Fock approach is used in all-electron calculations on bulk rutile (TiO_2) and various slabs modeling the (001), (100), and (110) surface to study possible geometric and electronic surface relaxations, convergence of properties with slab thickness, and the relative stability of the different surfaces. Results are discussed by means of a Mulliken population analysis, band structures, and the density of states. We find displacements of surface atoms ranging from 5 to nearly 40 pm; the (001) surface appears to be significantly unstable with respect to the other two [(100) and (110)], in accord with experimental findings. Specific features of the density of states projected onto different Ti sites and the relative stability of the different surfaces agree with a possible dissociation behavior of the rutile structure into TiO_2 chains, which are calculated to be stable.

I. INTRODUCTION

Titanium dioxide is an interesting compound because of its wide range of applications in catalysis, as sensor material and for coatings. From the theoretician's point of view, the presence of one of the lightest transition metals in nearly octahedral surroundings furnishes a reasonably complex system, yet amenable to *ab initio* calculations, due to the closed-shell unit cell with high symmetry. The moderate number of electrons per unit cell gives the opportunity to apply both all-electron treatments and effective core potentials with reasonably large basis sets.

The stoichiometric crystal is an ideal insulator with a reported electronic gap energy of 3.2 eV,[1-3] and experiments[4,5] indicate a significant hybridization of Ti $3d$ electrons with O $2p$, the latter dominating the valence-band density of states. The possible contributions of Ti and O to the valence band have been the subject of several publications, e.g., by Burdett[6] and Sorantin and Schwarz.[7] The different surfaces of rutile were studied by means of a Vos tight-binding Hamiltonian and the Green's functions method by Munnix and Schmeits.[8,9] The authors give an overview of the density of states modified by the presence of the surface for different bulk terminations, but without relaxation of the surface atom positions. Most recently, a paper by Podloutzky, Steinemann, and Freeman[10] showed first calculations employing the full-potential linear augmented-plane-wave (FLAPW) method on the geometric relaxation of the TiO_2 (110) surface aiming at an understanding of the adsorption of hydrogen. Relaxation of the (110) rutile surface has also been the subject of a study by Vogtenhuber *et al.*[11] However, these authors obtained substantially different results from ours.

The present paper will focus on the clean TiO_2 surfaces within a slab model by first reporting our calculations on bulk rutile (after a section briefly describing the method used), then showing results on different slabs and discussing and comparing properties. Differences in bond lengths of about 5 pm are difficult to observe with experimental techniques like x-ray photoelectron diffraction (XPD) or scanning tunnel microscopy but can change the electronic properties of the surfaces considerably; therefore, good *ab initio* data can shed some more light on the interesting features of rutile surfaces.

II. METHOD AND TECHNICAL DETAILS

For obtaining geometrical data, the Hartree-Fock method has been established as the most accurate and reliable method for the study of highly ionic compounds. The program CRYSTAL (Ref. 12) developed in Torino and Daresbury is an implementation of the Hartree-Fock scheme for periodic systems in zero to three dimensions based on the linear combinations of atomic orbitals forming crystal orbitals ansatz.[13,14] Bloch functions $\varphi_\omega(\mathbf{r};\mathbf{k})$ constructed from the set of Gaussian atomic orbitals of one reference unit cell $\chi_\omega(\mathbf{r})$ shifted to all unit cells by means of lattice vectors $\mathbf{g}$ are used as basis functions for the crystal one-electron orbitals $\psi_n(\mathbf{r};\mathbf{k})$ with expansion coefficients $c_{\omega n}(\mathbf{k})$

$$\psi_n(\mathbf{r};\mathbf{k})=\sum_\omega c_{\omega n}(\mathbf{k})\varphi_\omega(\mathbf{r};\mathbf{k}) ,$$

$$\varphi_\omega(\mathbf{r};\mathbf{k})=\sum_{\mathbf{g}} e^{i\mathbf{k}\cdot\mathbf{g}}\chi_\omega(\mathbf{r}-\mathbf{g})$$

maintaining the full translational symmetry of the infinite crystal and making use of the powerful integration algorithms used in molecular Hartree-Fock codes. The method and details of the implementation are well documented in the literature.[15]

For the practical work, the development of proper basis sets has to be considered first since the situation in a close-packed crystal is different from that of isolated molecules, for which satisfactory standard basis sets have been derived in the last 30 years. The use of very diffuse Gaussians and of polarization functions with low exponents can give rise to problems in crystal calculations due to linear dependencies caused by the regular arrays of the nuclei where the Gaussians are centered. We applied all-electron split-valence basis sets for Ti and O

TABLE I. Gaussian orbital exponents and total energy (in E_h) for optimized atomic basis sets (in parentheses the values optimized in the crystal).

	Ti	O
Single exponent 3*sp*		0.233 488 (0.244)
4*sp*	0.63 217 (0.793)	
5*sp*	0.00 553 (0.336)	
3*d*	0.37 597 (0.4052)	
E_{tot} our sets	848.259	74.7874
E_{tot} HF limit (Ref. 20)	848.406	74.8095

throughout this study. The use of effective core potentials is possible with CRYSTAL92, but, as known from molecular calculations, for the Ti atom the inclusion of the 3*sp* shell into the core must be done very carefully, as is stressed by Dolg *et al.*[16] Calculations should be compared to all-electron results with an explicitly frozen treatment of the core orbitals[17] with different core sizes. The all-electron basis set used for Ti was an 86411/6411/3 contraction (*s*/*p*/*d*) developed in Daresbury for the study of TiC,[18] of which we split the *d* contraction into 2-1 and reoptimized all single outer exponents in the experimentally found rutile structure. Oxygen was modeled by a basis set published by Causà *et al.* in a study of MgO,[19] namely an 861/61 contraction (8-61*G* since *s* and *p* orbitals share the same exponents). Optimized for atoms, these basis sets give total energies close to the Hartree-Fock limit[20] (Table I), although the number of Gaussian primitives is still moderate. For recent calculations on alkali oxides, a different oxygen basis set has been published[21] with a better 1*s* contraction. Structure and bulk moduli determined in this basis do not show significant deviations from results obtained with the oxygen basis set used in this study, although the total energy is slightly lower.

With these basis sets, we first optimized the structure of bulk rutile and used the resulting equilibrium geometry to cut slabs of different surfaces and different thickness. The optimization was restricted to explicit variations of the structural parameters by calculation of the total energy in some points and solving for the minimum of a polynomial or spline[22] fitted to these points.

Throughout the calculations presented here, the computational parameters defining the truncation criteria for the integration routines were set to values regarded as rather strict,[15] i.e., 5,5,5,5,11; convergence was always better than 10^{-6} a.u. for the eigenvalues or 10^{-8} a.u. for the total energy.

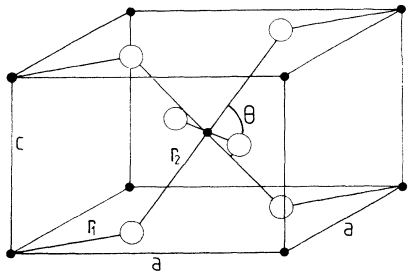

FIG. 1. The conventional unit cell of TiO_2 in its rutile structure and the defining parameters; Ti atoms are represented by black dots, the oxygen atoms by open circles.

III. CALCULATIONS ON BULK RUTILE

The rutile structure is quite common among transition-metal oxides and features a space group $P4/2mnm$ or D_{4h}^{14} with 16 symmetry operations and three independent lattice parameters to describe it completely (Fig. 1). One could choose, e.g., *a*, *c*, and *u* or the volume *V* and *c*/*a*, *u*, or the internal coordinates r_1, r_2, and Θ. The conventional unit cell comprises two TiO_2 units, giving a total number of 76 electrons in this cell. The structure is experimentally well investigated by x-ray diffraction[23] (room temperature) as well as neutron diffraction[24] (at 15 K), and also theoretical results can be found in recent literature [Hartree-Fock with effective-core potentials (ECP's)],[25] local-density approximation with ECP + plane waves,[26] and FLAPW (Ref. 7)] showing good agreement with the experimental lattice parameters.

For the determination of the equilibrium structure, we used the two bond lengths r_1, r_2, and the internal angle Θ as parameters expecting reasonably small coupling between these coordinates and thus making independent optimization possible: A variation of Θ affects Ti-Ti and O-O bonds, which are considered to be of minor importance to the structure.[27] After optimizing the angle Θ we searched for the best values of r_1 and r_2 and checked Θ again. The optimization was carried out using 75 *k* points in the irreducible wedge of the tetragonal first Brillouin zone. This procedure results in an estimated uncertainty of 0.2 pm for the bond lengths and 0.5° for Θ, leading to deviations from the experimental results within 2 pm and 2° (Table II), which we considered satisfactory. The good agreement is mainly due to the relatively high ionicity of the compound rendering electrostatic (Coulomb) and exchange interactions the main contribution to the binding energy; thus the neglect of correlation

TABLE II. Structure parameters and bulk modulus of rutile determined by various theoretical methods and comparison with experiment; we estimate the accuracy of our optimization procedure and the resulting fit of the minimum to ±0.2 pm and ±0.5°. Numbers in parentheses represent the deviations from experiment. For the experimentally determined bulk modulus, see the discussion in Ref. 26.

	r_1 (pm)	r_2 (pm)	Θ (°)	*B* (Mbar)
All-electron HF	196.5 (−1.1)	196.9 (+2.4)	100.5 (+1.7°)	2.81
Silvi *et al.* (Ref. 25)	197.2 (−0.4)	195.1 (+0.5)	100.4 (+1.6°)	
Glassford and Chelikowsky (Ref. 26)	200.7 (+3.1)	196.1 (+1.5)	98.25 (−0.6°)	2.40
Exp. (Ref. 24)	197.64	194.59	98.8	2.39

and the spin restriction is of minor importance. One qualitative difference to the experiment is that the order of r_1 (apical Ti-O bond length of the TiO_6 octahedron) and r_2 (equatorial bond length) comes out to be reversed, that is $r_1 < r_2$. Despite their smallness, the correlation contributions may be discussed in terms of the two most important mechanisms governing the details of the rutile structure. These are the repulsive interactions between the close-lying oxygen anions[28] in the equatorial octahedron plane (interatomic distance 2.571 Å) and a π-back-donation associated with the overlap of a metal d orbital with the oxygen p orbital, which lies perpendicular to the Ti_3 plane defined by each OTi_3 unit.[6,24] Both effects are underestimated in our calculations due to the neglect of electron correlation. We expect that the electron density in the outer valence shell of the anions is increased due to correlation[29] and thus the effective ion radius is enlarged, leading to a higher repulsion of the anions and a concomitant increase of the O Ti O angle. On the other hand, correlation will promote electron density from occupied orbitals into the unoccupied d orbitals, thus increasing the overlap population of the equatorial bond and shortening the bond length r_2 due to higher $p_O - d_{Ti}$ overlap.

In addition, we calculated the bulk modulus of rutile by fitting the total energy at different volumes to Murnaghan's equation of state[30,31]

$$E(V)=E(V_0)+\frac{VB}{B'(B'-1)}\left\{B'\left[1-\left[\frac{V_0}{V}\right]\right]+\left[\frac{V_0}{V}\right]^{B'}-1\right\}.$$

The two parameters B and B' could be determined very accurately from the data, but yield a value of $B=2.81$ MBar, off by 20% from the bulk modulus reported from experiments.[26] One has, of course, to allow for an anisotropic expansion or compression of the crystal, so that we varied the ratio c/a and the internal parameter u for fixed volume and searched over the range from 40 to 80 $Å^3$ for equilibrium geometries. As expected, keeping c/a and u constant as found at the equilibrium volume (isotropic variation) results in a bulk modulus significantly larger (3.09 MBar). Compared to the density-functional results of Glassford and Chelikowsky[26] and the experimentally observed value, the bulk modulus calculated with the Hartree-Fock method comes out to be too large, which is, in fact, a known feature of the method:[32] Inclusion of correlation is required to provide the necessary flexibility by relaxation of the strict spin correlation of a closed-shell Hartree-Fock procedure.

A Mulliken population analysis reveals that electrons remain centered at Ti atoms for the valence-band formation, reducing the ionicity of the crystal towards a +2.8 at Ti and −1.4 at oxygen. The bulk density of states shows a hybridization of Ti $3d$ and O $2p$ electrons over the whole valence band (Fig. 2), in agreement with experiments.[4] For calculation of the density of states (DOS) from the band structure, we used the quadratic analytical tetrahedron method of Wiesenekker and Baerends,[33] and te Velde.[34,35]

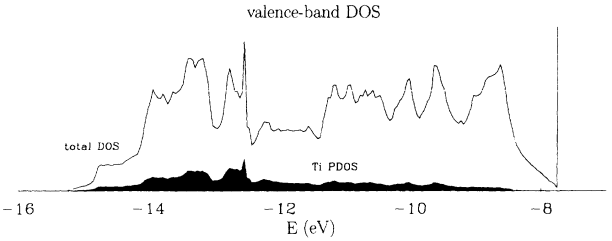

FIG. 2. Total density of states together with the projection onto the Ti atoms (black) for the completely filled valence band of bulk rutile. Hybridization extends over the whole region.

IV. THE SURFACE MODELS

From the equilibrium structure found for the bulk, we cut slabs of the (001), (100), and (110) surface with at least three Ti layers, of which the (100) and (110) surface have to be saturated with one additional oxygen atom per two-dimensional (2D) unit cell on each side of the slab to maintain the stoichiometry (Figs. 3 and 4). This oxygen is located in a twofold-coordinated site bridging two Ti atoms of the surface plane and can be expected to undergo a substantial relaxation due to electrostatical forces on the ions. For the (100) face, we therefore relaxed this atom on both sides of a three-layer slab while keeping the other positions fixed. More attention was paid to the (110) surface, since this is, according to the experiments, the only stable surface in contrast to the other two. Here we relaxed seven coordinates of the top layer independently. For a complete study of the unreconstructed (100) surface one also would have to optimize seven coordinates in the unit surface, but by actually moving just four atoms (the surface Ti in z direction, the top oxygen, and two oxygens underneath the surface Ti plane each in y and z direction). Cutting the (100) unit cell from the bulk leaves only four operators of the 16 of the bulk, reducing symmetry from D_{4h}^{14} to C_{2h}^{1} ($P2/m11$). The (110)

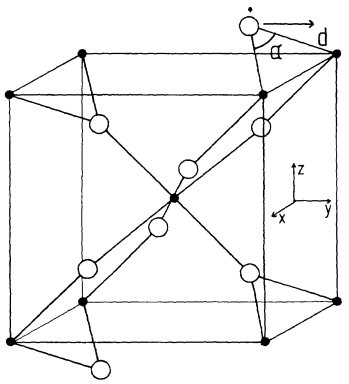

FIG. 3. The two-dimensional unit cell of a three-layer (100) slab together with definition of α and d. The topmost oxygen atom has been allowed to relax, the displacement is indicated.

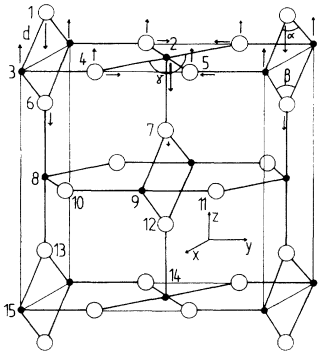

FIG. 4. The unit cell of the three-layer (110) slab with the enumeration of atoms used in the text; the octahedral surroundings of the Ti atoms can be clearly seen. Atom 3 is still sixfold coordinated while atom 2 has only five oxygen neighbors. Arrows showing the displacements of atoms due to the relaxation are multiplied by a factor of 5. In a five-layer slab, atoms 14 and 15 are in the middle plane of the slab.

surface, modeled by the slab, has still eight symmetry operations left and a symmetry of D_{2h}^{1} ($Pmmm$), but one has to consider two units of TiO_2 per layer instead of one for the (100) and the (001) surface. The (001) surface was treated as a sort of reference without any relaxation since it is documented that it is always reconstructed in different facets.[36] In all three cases, we used nine k points in the irreducible wedge of the two-dimensional rectangular first Brillouin zone.

Another special feature of the (110) surface is the good possibility to study the bonding properties of the transition-metal–oxygen octahedra since these are arranged with their apical axis in the surface plane or perpendicular to it giving the opportunity to divide the metal-d orbitals into e_g and t_{2g} ones in an easy way without a transformation of the coordinate system.

V. RESULTS AND DISCUSSION

We start the detailed discussion of our data with the (100) surface (see Table III): The bridging oxygen atom is shifted towards the titanium surface atoms increasing the Ti-O-Ti bond angle from 100.5° towards 109.7° and shortening the Ti-O bond from 196 to 185 pm. The angle between the plane of the Ti-O-Ti triangle and the slab is increased and in comparison with the bond shortening the displacement appears to be mainly lateral. Compared to the bulk ions, the top oxygen atom with the missing third Ti neighbor is a bit less negative and therefore the top Ti atom less positive. These features are also seen for the relaxation of the (110) surface, namely a top bond angle of 111.7°, a Ti-O bond length of 182.9 pm, and an occupation of 9.15 electrons instead of 9.38 for the bridging oxygen atom, according to a Mulliken analysis. In more detail, the fivefold-coordinated Ti atom (No. 2 as labeled in Fig. 4) tends to move into the slab due to electrostatic forces by nearly the same displacement of 14.6 pm as the top oxygen (1). This movement is passed to the underlying ions (6 and 7) displacing them by 7.2 and 2.3 pm, respectively, in the same direction. The sixfold-coordinated surface titanium atom (3) is found in a stable position 9.2 pm outwards, the oxygen atoms 4 and 5 (equivalent by symmetry) follow with a shift of 6.6 pm outwards. The latter ions were also displaced laterally to be found in an optimum position 7.5 pm further away from the surface titanium atom 3.

TABLE III. Relaxation of the (100) surface (top oxygen displaced only). α and d as in Fig. 3.

Δy		38.8 pm
Δz		4.4 pm
α	100.5°	109.7°
d	196.5 pm	185.0 pm
E_{tot}	−2994.833 a.u.	−2994.882 a.u.
$Q_{\text{top } O}$	−1.230 e	−1.162 e

The (cumbersome) procedure of optimization was done by displacements for the two sides of the slab maintaining the symmetry of the unrelaxed slab. The only nonoptimized coordinate is, therefore, the lateral position of the oxygen atoms in the middle layer of our three-layer slab (atoms 10 and 11). Since the displacements of the atom next to the middle plane (7) is only 2.4 pm, we think, that further improvements will give only minor changes of the reported displacements. Moreover, increasing the size of the slab to a five-layer model will result in the same data as compiled in Table IV. For calculations on the highly ionic compounds MgO (Ref. 37) or LiH (Ref. 38), it has been shown that convergence of properties with the slab thickness is reached with a small number of layers, a point to be investigated[39] in all slab calculations as well as in cluster approaches. Table V, therefore, gives the Mulliken charges for slabs of different thickness for the (100) and the (110) surface. According to these data, a five-layer slab is in both cases sufficient to have bulk properties in the interior of the two-dimensional model, but one could use already a three-layer slab to study, e.g., weak adsorption situations since the charges of the topmost atoms remain nearly constant. Additionally, we present the density of states (Fig. 5), projected onto the two innermost Ti atoms of the five-layer (110) slab, in comparison to the bulk density of states of Ti. The contributions to the O 2s, the valence band (O 2p), and the unoccupied Ti 3d bands are displayed showing excellent agreement not only on the bandwidths, but also of the major bulk features. This looks even more satisfying when noticing the different orientation of the corresponding octahedra with respect to the surface of the slab.

Along with bond-length shortening for the top Ti-O bond, one could expect also an influence on the total valence-band width in the course of the relaxation, but here we see that the valence band becomes narrower instead of broadening, showing the still high ionicity of the compound. The strong surface feature at the Fermi level is slightly moderated and hybridization with the other orbitals of the slab increase (Fig. 6). For the (110) slab, the main contribution to the valence-band DOS of the unrelaxed surface derived from the topmost oxygen is shared

TABLE IV. Relaxation of the (110) surface. The enumeration of atoms and α, β, γ, and d as in Fig. 4.

Atom	1	2	3	4,5	6	7	4,5 in y direction
Type	O	Ti	Ti	O	O	O	O
Δz	−14.0	−14.6	+9.2	+6.6	−7.2	−2.3	±7.5
α	100.5°	111.7°					
β	100.5°	93.5°					
γ	180.0°	167.4°					
d	196.5 pm	182.9 pm					
E_{tot}	−5989.808 a.u.	−5989.895 a.u.					
$Q_{top\ O}$	−1.250 e	−1.145 e					

TABLE V. Ion charges according to a Mulliken population analysis.

	Three layers unrelaxed	Three layers	Five layers	Seven layers	Bulk
		Rutile (100) surface			
Top O	−1.230	−1.162	−1.163	−1.163	−1.377
Top Ti	+2.611	+2.574	+2.573	+2.573	+2.754
Second-layer Ti	+2.748	+2.745	+2.749	+2.749	
Third-layer Ti			+2.754	+2.754	
Fourth-layer Ti				+2.754	
		Rutile (110) surface			
Top O	−1.250	−1.145	−1.141		−1.377
Ti (2)	+2.690	+2.637	+2.635		+2.754
Ti (3)	+2.655	+2.629	+2.627		
Second-layer Ti (8)	+2.749	+2.725	+2.737		
Ti (9)	+2.749	+2.747	+2.750		
Third-layer Ti (14)			+2.754		
Ti (15)			+2.754		

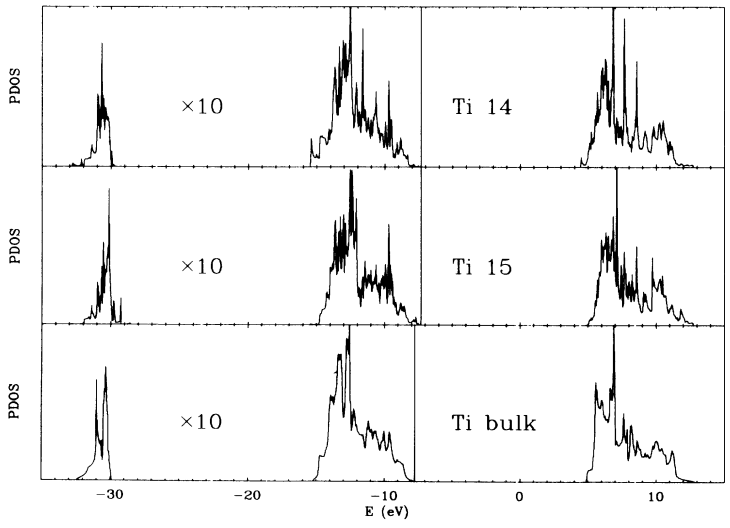

FIG. 5. The density of states of the five-layer (110) slab projected onto the two innermost Ti atoms (14 and 15 as in Fig. 4) together with the bulk DOS projected onto the Ti contributions. For the O 2s and the O 2p, band the contributions are multiplied with a factor of 10. The origin of the energy scale has been adjusted at the Ti 1s orbital energies.

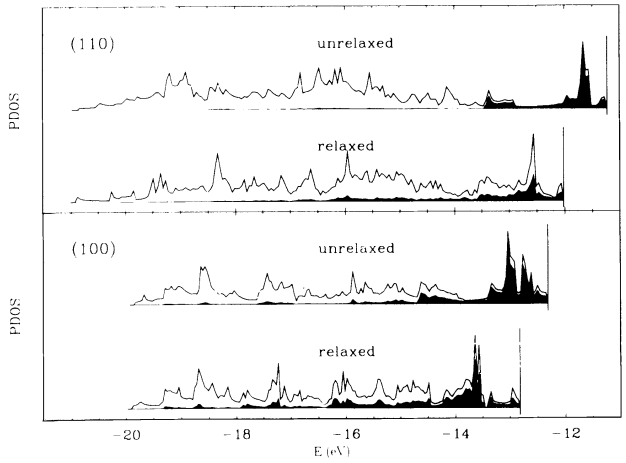

FIG. 6. Effect of the relaxation on the valence-band density of states of the specific three-layer slabs of the (100) and the (110) surface. The total DOS is displayed together with the DOS projected onto the topmost oxygen atom (black). Although bond lengths are shortened, the bandwidth is not broadened by the relaxation.

after the relaxation with the oxygen atom underneath (6), making the total valence-band DOS look more compact. The lower edge of the valence band is in both cases [(100) and (110)] not affected by the displacement of the surface atoms. In Fig. 7, we display the valence-band DOS for the relaxed surfaces in comparison to the one from the (001) slab and bulk rutile; the energy scale has been adjusted at the Ti 1*s* orbital energy of the interior of the slabs or the bulk, respectively. Apparently, the (110) valence-band width is significantly larger than that of the three other objects (8.5 instead of 7.5 eV), of which the width is quite similar.

TABLE VI. Surface energy per TiO_2 according to $\frac{1}{2}([E_{tot}^{bulk}/TiO_2 - E_{tot}^{slab}/TiO_2]$ times the number of layers) for the three surfaces studied.

		E_{tot}/TiO_2 (a.u.)	$E_{surf.}/TiO_2$ (a.u.)
bulk		−998.346	
(0 0 1)			
	Three layers[a]	−998.205	0.2113
	Five layers[a]	−998.262	0.2110
(1 0 0)			
	Three layers[a]	−998.278	0.1021
	Three layers	−998.294	0.0772
	Five layers	−998.315	0.0776
	Seven layers	−998.323	0.0790
(1 1 0)			
	Three layers[a]	−998.301	0.0664
	Three layers	−998.316	0.0453
	Five layers	−998.327	0.0467

[a]Slab cut from bulk without relaxation.

Table VI gives the total energy per TiO_2 and the differences to the bulk value to obtain an estimate of the surface formation energy. To calculate this value, one has to account for the number of TiO_2 units created at the surface versus the number of units contained in the 2D unit cell. In agreement with the experimental observation, the (100) and the (001) surfaces are less stable than the (110) surface. It is known that the (100) surface reconstructs after heating into 1×3, 1×5, and even 1×7 structures with microfacets of (110) orientation.[40,41] The (001) surface is unstable.

The band structure plotted for the relaxed five-layer slab including the O 2*s* bands, the valence band, and the first unoccupied states (Fig. 8) shows the convergence of surface features with the slab thickness, too. Looking at

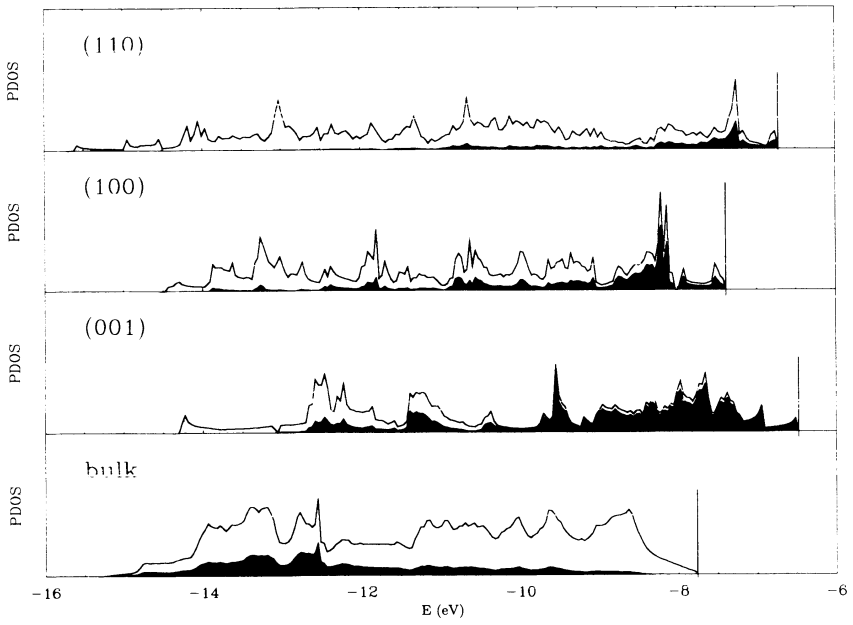

FIG. 7. Comparison of the valence-band density of states for bulk and the three surfaces (three-layer slabs) studied. The origin of the energy scale has been adjusted according to the Ti 1*s* orbital energy of the innermost Ti level of a five-layer slab. The (110) and (001) valence-band width are the same as for the bulk, whereas the (110) surface exhibits a significant broadening due to the different chemical surroundings of the two inequivalent surface Ti atoms. As in Fig. 6, the total density of states is displayed together with the contributions of the topmost oxygen atoms (black, Ti in the case of bulk rutile).

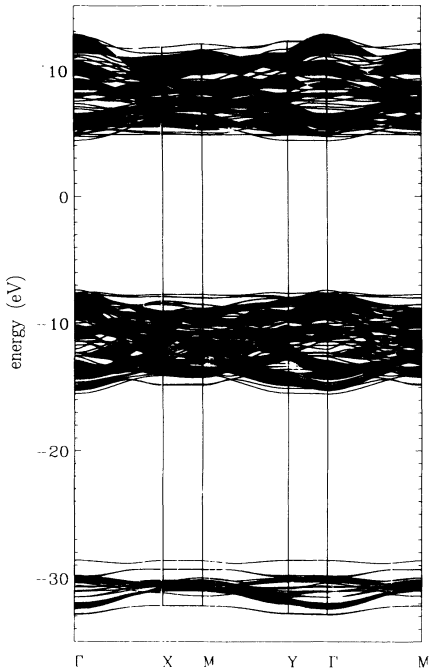

FIG. 8. Band structure of the five-layer (110) slab together with the surface projection of the bulk bands (shaded area) to show the specific surface contributions. The surface-induced core-level shifts (O 2*s* bands) can be seen clearly while the other bands fit well to the bulk bands.

the O 2*s*-like bands, one can see three eigenvalues derived (upper to lower) from the oxygens (1), (6), and (7) orbitals. The contributions from the surface oxygen atoms on either side of the slab turn out to be degenerate, as they should be for independent surfaces. Calculations on a three-layer slab gave still a splitting of these levels of 0.2 eV—1 eV at the Γ point.

To see the reason for the valence-band broadening for the (110) slab compared to the others, we looked at the density of states projected onto the different Ti contributions to the total valence-band DOS (Fig. 9). Clearly, there is a difference for the two surface atoms. Also the atoms of the next layer (Ti 8 and 9) are far from equivalent but, for the innermost Ti atoms, we see only little extra contributions on either side of the (main) valence band. This points towards some surface states decaying in amplitude exponentially when tracing them into the bulk material. The sixfold-coordinated surface Ti atom is more involved in the occurrence of the additional feature near the Fermi level, because the electrons of the topmost oxygen are distributed over two Ti neighbors instead of three as in the bulk. On the other hand, the missing oxygen neighbor of the fivefold-coordinated surface Ti leaves the density of states projected onto it rather unchanged. A comparison of the five *d* levels of the fivefold-coordinated surface Ti atom and the bulk Ti, equally orientated, gives a poignant contribution for the equatorial e_g-like orbital (d_{xy} in our case) and a distributed one for the other ($d_{3z^2-r^2}$), while the t_{2g} orbitals ($d_{xz}, d_{yz}, d_{x^2-y^2}$) remain only weakly occupied (Fig. 10). The relatively small dispersion of the d_{xy}-derived bands lead us to look at a possible dissociation of bulk rutile in order to study the stability of the equatorial Ti-O bonds. The closed-shell Hartree-Fock is expected to be capable of this problem, because the resultant objects have still a closed-shell unit cell. To this end, we extended the calculations at fixed volumes (as we did for obtaining the bulk modulus) to 100, 120, 400, and 10 000 Å^3 and plotted the two resultant Ti-O bond lengths against the volume in Fig. 11. According to this r_2 tends to go to a constant value, while r_1 grows with the volume, asymptotically to $\sqrt{V/2c}$. The optimum bulk volume is near the intersection of the two curves (r_1 and r_2), so the equilibrium between the Ti-O bond lengths is quite subtle.

As is seen from the rutile structure in Fig. 1, a constant r_2 together with a growing r_1 leads to chains of TiO_2 units (Fig. 12) running parallel in *z* direction, and in the case of the (100) and (110) surface, parallel to the slabs studied. The question to be considered next is that whether the situation at the surfaces is similar to that of isolated chains, at least for the geometric relaxation. This could also, as for the slab thickness, lead to an estimate of the range of ordering forces.

The polymer chain was treated in two ways: first we held the spacing of Ti atoms fixed at the value found for bulk rutile ($c = 3.026$ Å), since the 2D periodicity forces the chains at the surfaces into this mesh. The one free parameter to be optimized was, in this case, the angle Θ giving a value significantly larger than in bulk rutile (Table VII). Leaving the 1D grid parameter free, the chain is contracted a little (5%), while the angle goes back to nearly 100°. Bond lengths are in all cases listed smaller than the bulk value, also the charge of the participating oxygen is less negative, mainly because the third Ti neighbor is either farther away or missing. Looking at the total energy in Table VII, one can see that the TiO_2 polymers are still bound objects with respect to the free atoms.

Exactly this is in accordance with the relative stability of the three surfaces studied (Table VII), because in the case of the (001) surface the stabilizing chains are cut, but they are conserved for the two other surfaces. The Ti-O bond lengths are in good agreement for the polymers and the surfaces. The same holds for the internal angle Θ, which is larger than in the bulk.

VI. SUMMARY

We employed the all-electron periodic Hartree-Fock approach to calculate structural parameters, band structure, and density of states for rutile surfaces modeled by means of a slab cut from an ideal crystal. Structural parameters for the bulk are obtained in good agreement with experiment and previous theoretical work. Significant geometrical relaxation is found in the surface models as compared to the bulk geometry, mainly due to the high ionicity of the compound. Convergence to bulk properties can be seen within a five-layer slab both for a Mulliken analysis and for the local density of states (DOS projected onto inner atoms). From the surface energy of the different slabs and from the anisotropy of the bulk

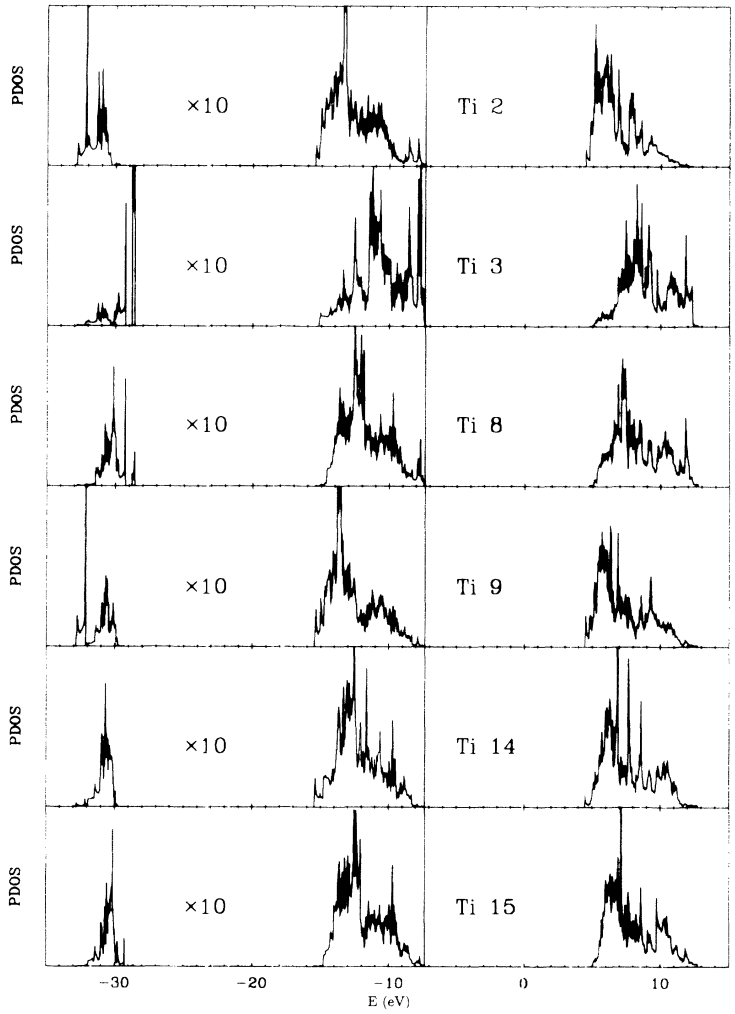

FIG. 9. Density of states of the relaxed five-layer (110) slab projected onto the different Ti atoms. The contributions to the O 2*s* and O 2*p* (valence) band have been multiplied by a factor of 10.

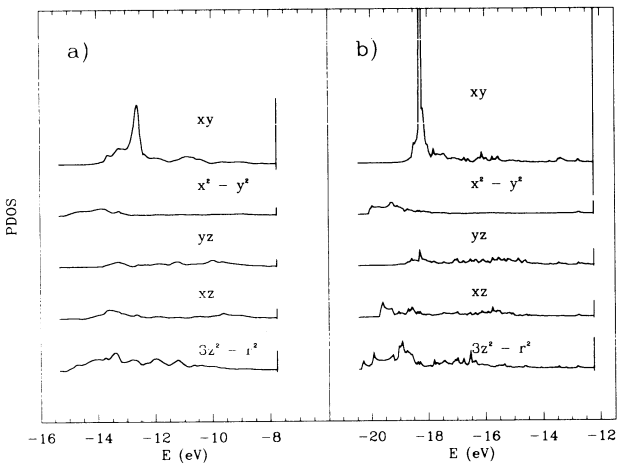

FIG. 10. (a) Projection of the density of states onto the five *d* orbitals of the fivefold-coordinated surface Ti atom (2), the main contribution to the total density of states coming from the d_{xy} orbital. (b) Bulk density of states projected onto the Ti *d* orbitals. To make the comparison possible, the unit cell has been rotated and orientated as the (110) unit cell. The projection is onto the Ti atom with the apical axis along the coordinate *z* axis.

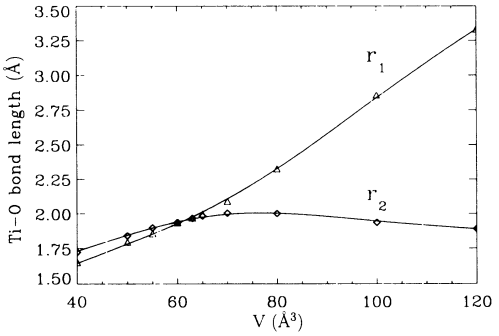

FIG. 11. Internal bond lengths r_1 and r_2 at equilibrium structures for different fixed volumes *V*. The intersection of the two curves is nearly at the volume found by means of the optimization procedure for the bulk.

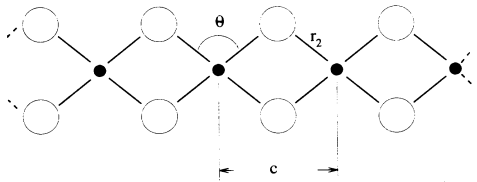

FIG. 12. The TiO_2 polymer studied. The optimization was carried out using the parameters r_2 and Θ; for fixed unit-cell length *c* (at the length given through the slabs) we varied the angle Θ.

TABLE VII. Geometrical study of the TiO_2 chains. We compared the data for the two polymers (c fixed and free), the two slabs (110) and (100), and the bulk. The total energy for the free atoms is given for comparison (see Table I). Parameters that have been kept fixed are denoted by numbers in parentheses.

	c (Å)	Ti-O (pm)	Θ	$Q_{Ox.}$	E_{tot}/TiO_2 (a.u.)
TiO_2 polymer (1)	(3.026)	189.9	105.6°	−1.162	−998.138
TiO_2 polymer (2)	2.880	185.9	101.2°	−1.109	−998.146
(100) surface	(3.026)	185.0	109.7°	−1.162	
(110) surface	(3.026)	182.6	111.7°	−1.145	
Bulk at 10000 Å^3	2.879	185.5 (r_2)	101.8°	−1.185	−998.139
Bulk	3.026	196.5 (r_2)	100.5°	−1.377	−998.346
Free atoms					−997.812

modulus, we conclude that the equatorial Ti-O bond is more stabilizing than the apical one, giving rise to a hypothetical dissociation of rutile into TiO_2 chains, thus providing a simple model explaining the relative stability of the various TiO_2 surfaces.

ACKNOWLEDGMENTS

This work was supported by the 'Deutsche Forschungsgemeinschaft' via SFB 334 and by the 'Fonds der Chemischen Industrie'. Computer resources and support of the HLRZ in Jülich are gratefully acknowledged. We should like to thank V. R. Saunders for making his Ti basis set available to us and R. Dovesi for helpful discussions. The copy of the Amsterdam Density-Functional program BAND kindly supplied by G. te Velde and E. J. Baerends was instrumental for obtaining the density of states in the framework of the quadratic tetrahedron method. P.R. gratefully acknowledges the kind support by G. te Velde and K. Wandelt, Bonn.

[1]N. I. Medevedeva, V. P. Zhukov, M. Y. Khodos, and V. A. Gubanov, Phys. Status Solidi B **160**, 517 (1990).
[2]J. Pascual, J. Camassel, and H. Mathieu, Phys. Rev. B **18**, 5606 (1978).
[3]W. Göpel, J. A. Andersen, D. Frankel, M. Jaehnig, K. Phillips, J. A. Schäfer, and G. Rocker, Surf. Sci. **139**, 333 (1984).
[4]R. Heise, R. Courths, and S. Witzel, Solid State Commun. **84**, 599 (1992).
[5]Z. Zhang, S.-P. Jeng, and V. Henrich, Phys. Rev. B **43**, 12 004 (1991).
[6]J. K. Burdett, Inorg. Chem. **24**, 2244 (1985).
[7]P. Sorantin and K. Schwarz, Inorg. Chem. **31**, 567 (1992).
[8]S. Munnix and M. Schmeits, Phys. Rev. B **30**, 2202 (1984).
[9]S. Munnix and M. Schmeits, J. Vac. Sci. Technol. A **5**, 910 (1987).
[10]R. Podloutzky, S. G. Steinemann, and A. J. Freeman, New J. Chem. **16**, 1139 (1992).
[11]D. Vogtenhuber, R. Podloutzky, A. Neckel, S. G. Steinemann, and A. J. Freeman, Phys. Rev. B **49**, 2099 (1994).
[12]R. Dovesi, C. Pisani, C. Roetti, M. Causà, and V. R. Saunders, CRYSTAL88, *An Ab Initio All-Electron LCAO Hartree-Fock Program for Periodic Systems,* Quantum Chemistry Program Exchange (QCPE) #577 (1989); R. Dovesi, V. R. Saunders, and C. Roetti, CRYSTAL92 User Documentation, Torino and Daresbury (1993).
[13]J. M. André, L. Gouverneur, and G. Leroy, Int. J. Quantum. Chem. **1**, 517 (1967).
[14]G. DelRe, J. Ladik, and G. Biczò, Phys. Rev. **155**, 997 (1967).
[15]C. Pisani and R. Dovesi, Int. J. Quantum. Chem. **17**, 501 (1980); C. Pisani, R. Dovesi, and C. Roetti, *Hartree-Fock Ab Initio Treatment of Crystalline Systems,* Lecture Notes in Chemistry Vol. 48 (Springer-Verlag, Heidelberg, 1988).
[16]M. Dolg, U. Wedig, H. Stoll, and H. Preuss, J. Chem. Phys. **86**, 866 (1987).
[17]P. Reinhardt and B. A. Heβ (unpublished).
[18]V. R. Saunders (private communication).
[19]M. Causà, R. Dovesi, C. Pisani, and C. Roetti, Surf. Sci. **175**, 551 (1986).
[20]S. Fraga, J. Karwowsky, and K. M. S. Saxena, *Handbook of Atomic Data* (Elsevier, Amsterdam, 1976), p. 141.
[21]R. Dovesi, C. Roetti, C. Freyria-Fava, and M. Precipe, J. Chem. Phys. **156**, 11 (1991).
[22]C. H. Reinsch, Numer. Math. **10**, 177 (1967).
[23]S. C. Abrahams and J. L. Bernstein, J. Chem. Phys. **55**, 3206 (1971).
[24]J. K. Burdett, T. Hughbanks, G. J. Miller, J. W. Richardson, and J. V. Smith, J. Am. Chem. Soc. **109**, 3639 (1987).
[25]B. Silvi, N. Fourati, R. Nada, and C. R. A. Catlow, J. Phys. Chem. Solids **52**, 1005 (1991).
[26]K. M. Glassford and J. R. Chelikowsky, Phys. Rev. B **46**, 1284 (1992).
[27]M. Sakata, T. Uno, M. Takata, and R. Mori, Acta Crystallogr. Sec. B **48**, 591 (1992).
[28]M. O'Keeffe, Acta Crystallogr. Sec. A **33**, 924 (1977).
[29]B. A. Heβ, H. L. Lin, J. E. Niu, and W. H. E. Schwarz, Z. Naturforsch. **48a**, 180 (1993).
[30]F. D. Murnaghan, Proc. Natl. Acad. Sci. U.S.A. **30**, 244 (1944).
[31]O. L. Anderson, J. Phys. Chem. Solids **27**, 547 (1966).
[32]E. Aprà, M. Causà, M. Prencipe, R. Dovesi, and V. R. Saunders, J. Phys. Condens. Matter **5**, 2969 (1993).
[33]G. Wiesenekker and E. J. Baerends, J. Phys. Condens. Matter **3**, 6721 (1991).
[34]G. te Velde, Ph.D. thesis, Vrije Universiteit, Amsterdam,

1990.
[35]G. te Velde and E. J. Baerends, Phys. Rev. B **44**, 7888 (1991).
[36]G. E. Poirier, B. K. Hance, and J. M. White, J. Vac. Sci. Technol. B **10**, 6 (1992).
[37]R. Dovesi, R. Orlando, F. Ricca, and C. Roetti, Surf. Sci. **186**, 267 (1987).
[38]M. Causa, R. Dovesi, and F. Ricca, Surf. Sci. **237**, 312 (1990).
[39]G. te Velde and E. J. Baerends, Chem. Phys. **177**, 399 (1993).
[40]Y. W. Chung, W. L. Lo, and G. A. Somorjai, Surf. Sci. **64**, 588 (1977).
[41]G. W. Clark and L. L. Kesmodel, Ultramicroscopy **41**, 77 (1992).